Journal of Power Sources 243 (2013) 611–616

Contents lists available at SciVerse ScienceDirect

Journal of Power Sources

journal homepage: www.elsevier.com/locate/jpowsour

Short communication

Influence of the thickness of the capacitive layer on the performance of bioanodes in Microbial Fuel Cells

Alexandra Deeke [a,b,*], Tom H.J.A. Sleutels [b], Annemiek Ter Heijne [a], Hubertus V.M. Hamelers [b], Cees J.N. Buisman [a,b]

[a] Sub-Department of Environmental Technology, Wageningen University, Bornse Weilanden 9, P.O. Box 17, 6708 EG Wageningen, The Netherlands
[b] Wetsus, Centre of Excellence for Sustainable Water Technology, Agora 1, P.O. Box 1113, 8900 CC Leeuwarden, The Netherlands

HIGHLIGHTS

- Storage of electricity produced by MFC possible with integrated capacitive bioanode.
- Thickness of the capacitive layer is influencing the performance of the MFC.
- Capacitive layer with a thickness of 0.2 mm was found to be the most efficient.
- Increase of 40% during intermittent operation compared to continuous operation of a noncapacitive electrode.

GRAPHICAL ABSTRACT

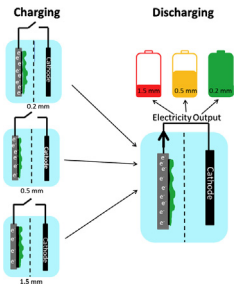

ARTICLE INFO

Article history:
Received 18 March 2013
Received in revised form
14 May 2013
Accepted 24 May 2013
Available online 12 June 2013

Keywords:
Microbial Fuel Cell
Capacitive electrode
Relative charge recovery
Intermittent operation

ABSTRACT

Earlier it was shown, that it is possible to operate a Microbial Fuel Cell with an integrated capacitive bioanode with a thickness of 0.5 mm and thereby to increase the power output. The integrated capacitive bioanode enabled storage of electricity produced by microorganisms directly inside an MFC. To increase the performance of this integrated storage system even more; the thickness of the capacitive electrode was varied: 0.2 mm, 0.5 mm and 1.5 mm. Each of these capacitive electrodes was tested in the MFC setup during polarization curves and charge–discharge experiments for the steady-state current density and the maximum charge recovery.

The capacitive electrode with a thickness of 0.2 mm outperformed the other electrodes in all experiments: it reached a maximum current density of 2.53 Am^{-2} during polarization curves, and was able to store a cumulative total charge of 96013 cm^{-2} during charge–discharge experiments. The highest relative charge recovery for this electrode was 1.4, which means that 40% more current can be gained from this capacitive electrode during intermittent operation compared to continuous operation of a noncapacitive electrode. Surprisingly it was possible to increase the performance of the MFC through decrease of the thickness of the capacitive electrode.

1. Introduction

Energy production from renewable sources receives more and more attention due to the depletion of fossil fuels and the increasing pollution of the atmosphere. Most of this attention is focused on solar and wind energy [1]. But there are also an

* Corresponding author. Sub-Department of Environmental Technology, Wageningen University, Bornse Weilanden 9, P.O. Box 17, 6708 EG Wageningen, The Netherlands. Tel.: +31 58 2843190; fax: +31 58 2843001.
E-mail address: Alexandra.Deeke@wetsus.nl (A. Deeke).

0378-7753/$ – see front matter © 2013 Elsevier B.V. All rights reserved.
http://dx.doi.org/10.1016/j.jpowsour.2013.05.195

increasing number of researchers looking at possibilities to use biomass as a renewable energy source [2]. One type of biomass, which is not yet used in the most efficient way, is wastewater. So far, most wastewater treatment plants spend energy to remove the organic compounds contained in wastewater. But recently there has been developed a more efficient technology: the Microbial Fuel Cell (MFC). In MFCs the organic compounds of the wastewater are directly converted into electricity [3]. An MFC consists of an anode compartment and a cathode compartment, which are usually separated by a membrane [4]. Both compartments contain an electrode; the anode and cathode. On the anode grow electrochemically active microorganisms which convert the organic matter from wastewater into protons, electrons and carbon dioxide. Positively charged ions migrate through the membrane (in case of a cation exchange membrane) to the cathodic compartment and the electrons are transported through an external circuit to the cathode. At this cathode the protons and electrons react with oxygen to form water [5].

The MFC is thereby presenting a way of simultaneously treating wastewater and producing electricity. However, the wastewater needs to be treated continuously and the energy which is produced by the MFC might not be consumed continuously. To match the production and demand of this electricity, storage of the electricity would be necessary [6]. Two different techniques have been investigated for the storage of electricity from MFCs: external and internal capacitors [7–12]. Dewan et al. [7] and Kim et al. [8], Grondin et al. [9], Liang et al. [10] and Hatzell et al. [11] showed that using a Bio Electrochemical System (BES) with an external capacitor can improve the power output compared to continuous operation of the BES without capacitor. Another way of increasing the power output of MFCs was shown by Deeke et al. [12]. They operated the MFC with a capacitor integrated in the anode compartment, and also found an increase in power output. Until now, however, it is not known which parameters determine the performance of the MFC with a capacitor.

Several studies in the field of electricity storage in capacitors have shown that the specific capacitance is, amongst others, depending on the thickness of the active material of the electrodes [13,14]. Emmenegger et al. [13] compared the specific capacitance of electrodes used in electrochemical double-layer capacitors, which were made of Activated Carbon Powder (ACP) in 6 different thicknesses varying from 0.1 mm to 0.8 mm. They found an increase in the specific capacitance, when increasing the thickness of the active material. Tsay et al. [14] tested four different thicknesses for their supercapacitor electrodes: 0.05 mm, 0.1 mm, 0.2 mm and 0.3 mm. They found an optimum in the specific capacitance for their electrodes at a thickness of 0.1 mm.

To further improve the performance of MFCs with an internal capacitive bio-anode, we compared three different thicknesses for the capacitive layers: 0.2 mm, 0.5 mm and 1.5 mm. The performance of the layers with different thickness was analyzed using polarization curves and charge–discharge experiments to see the steady-state current density and the maximum charge recovery in a two chamber MFC.

2. Materials and methods

2.1. Electrochemical cell setup

In this study, six identical cells were used to characterize the performance of the different capacitive layers. The six cells were similar to the ones used in the proof of concept study of the internal capacitive bioanode [12]. The cells consisted of two flow channels of each 33 mL for the anodic and cathodic compartment. The flow channels were separated by a Cation Exchange Membrane (Ralex, Mega, Straz pod Ralskem, Czech Republic) and on both sides of the membrane the electrodes (Müller & Rössner GmbH, Troisdorf, Germany) were placed. The cathode electrode was a noncapacitive (plain graphite plate) electrode and the anode was a current collector (plain graphite plate) covered with the capacitive layer. Anode, cathode and membrane had a projected surface area of 22 cm^2 each.

2.2. Electrode preparation

The capacitive layers were prepared by mixing a pre-mixed PVDF-solution; 200 mL NMP (N-methyl-2-pyrrolidone, Boom, Meppel, The Netherlands) and 44.1 g PVDF (Polyvinylideenfluoride 2, Kynar, Arkema, Amersfoort, The Netherlands) with 25.2 g of Activated Carbon Powder (ACP, DLC Super 30, Norit, Amersfoort, The Netherlands). A scheme of the preparation of the capacitive electrodes is in Fig. 1.

This solution was placed in a ball-mill grinder (PM 100, Retsch, Haan, Germany) and mixed at 450 rpm for 30 min. Afterward the capacitive paint was kept in an oven for 24 h at 50 °C for deaeration. The capacitive paint was casted in three different thicknesses on the current collector using a casting knife. The thicknesses of the tested electrodes were, 0.2 mm, 0.5 mm and 1.5 mm. Each electrode was casted in triplicate.

Each capacitive electrode was analyzed using several techniques: BET-Analysis, AFM and SEM pictures The specific surface area of the capacitive electrodes was determined using the BET-Analysis [15]. The roughness of each capacitive electrode was determined using atomic force microscope (AFM, Nanoscope Illa, Veeco, Santa Barbara, CA, USA). The AFM-scan was performed on 1 mm^2 of the surface area. The roughness of the scanned surface area was determined using the AFM [16] as the arithmetic average R_a of the absolute roughness values of the surface of each capacitive

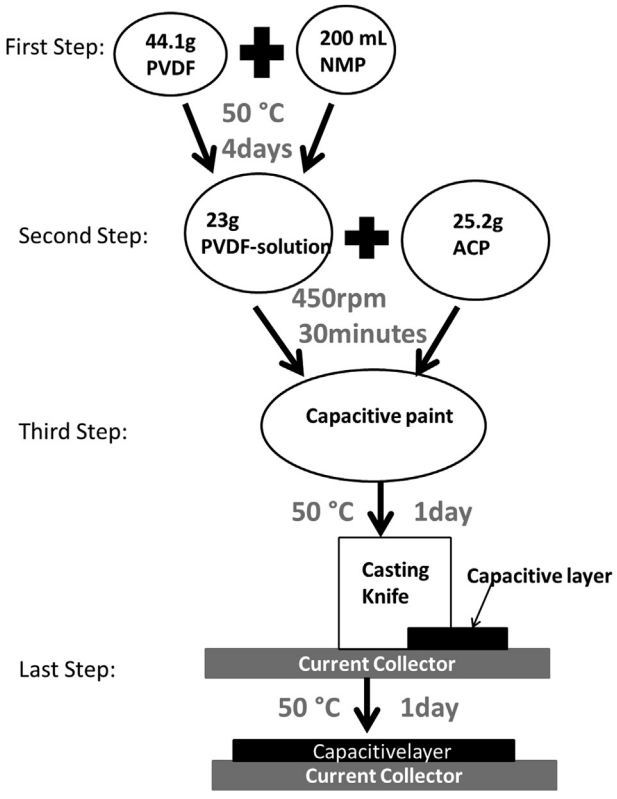

Fig. 1. Preparation of the capacitive layers from the beginning till the end.

layer. The pore-size distribution on the surface was determined using SEM (Scanning Electron Microscope, JEOL Technics Ltd., Tokyo, Japan). AFM-scans and SEM-pictures were taken on three different positions of each capacitive electrode to get a representative overview.

2.3. Operation and measurements

The MFCs were fed with synthetic wastewater containing 10 mM of sodium acetate and 10 mM of phosphate buffer. New influent was supplied at a rate of 1.3 mL min^{-1} and recirculated over a storage vessel with a rate of 100 mL min^{-1} using peristaltic pumps (Master Flex, Cole Parmer, Vernon Hills, IL, USA). A Vitamin solution, Micro- and Macronutrients were added to the anolyte with 1 mL L^{-1}, 1 mL L^{-1} and 10 mL L^{-1}. The composition of the Nutrient-solutions can be found in Ref. [17]. The catholyte was a 10 mM potassium-ferricyanide solution, which was supplied to the MFCs at a rate of 100 mL min^{-1}. The temperature of each cell was controlled at 30 °C with a water bath (K10, Thermo scientific, Geel, Belgium). The pH in the anode compartment was constantly measured using a pH-electrode (Liquisys, Endress + Hauser, Naarden, The Netherlands).

The cells were operated at a controlled anode potential with a potentiostat (N-stat, Ivium Technologies, Eindhoven, The Netherlands). The anode potential was set to −0.400 V (vs. Ag/AgCl + 0.2 V vs. NHE), Pro Sense, Oosterhout, The Netherlands)(demonstrated as an optimal working potential for the microorganisms during earlier research [18]) unless stated otherwise. Current and anode potential were measured constantly.

The cells were operated for 120 days, during these days of operation polarization curves and charge–discharge experiments were performed. All capacitive layers were tested in duplicate.

Polarization curves were performed to determine the maximum current density output of the capacitive electrodes. The polarization curves were recorded at day 32, 76 and 120 of operation. During the polarization curves the anode potential was varied from −0.450 V to −0.250 V in steps of 0.050 V. Each potential was held for 10 min till the cell reached a stable current output. The current density output for each potential was taken from the average for the last minute at each potential.

During the charge–discharge experiments; periods of operation at open circuit conditions (charging) were alternated with periods of operation at a set anode potential (discharging) of −0.300 V (this potential was chosen according to the maximum current density of the noncapacitive electrode [12]). The periods for charging and discharging were varied to determine the maximum charge capacity of the capacitive electrodes. The different charge and discharge periods which have been used are in Table 1.

2.4. Calculations

The current density was calculated from the measured current divided by the surface area of the anode as $i = I/A$ in Am^{-2}.

To evaluate the performance of each capacitive electrode during the charge–discharge experiments the cumulative total charge was calculated. The cumulative total charge is represented by the surface area of the current density-curve of a charge–discharge experiment. Therefore the cumulative total charge can be calculated as

$$Q_m = \int i_m \mathrm{d}t \quad (1)$$

where Q_m is the charge measured during the discharge period (measured charge) and i_m is the current measured during the discharge period. The measured charge consists of two different parts: the current which is produced and retrieved directly from the bio-electrode and the stored charge, which was delivered from the microorganisms to the capacitive electrode during the charging period. This means that the measured charge can also be expressed as;

$$Q_m = i_p(t_o - t_c) + Q_s \quad (2)$$

where i_p is the current produced by the microorganisms, t_o is the overall time of the charge–discharge experiment, t_c is the charging time and Q_s is the charge stored during the charging period.

To evaluate the efficiency of these capacitive electrodes the cumulative total charge of each experiment is related to the charge, which could have been extracted from a noncapacitive electrode during continuous operation. The charge for continuous operation is calculated according to; $Q_{cont} = i_{nc}{}^{*}t_o$, where Q_{cont} is the charge of continuous operation, i_{nc} is the current measured for the noncapacitive electrode at an anode potential of −0.300 V (1.74 mA) and t_o is the overall charge–discharge time. Relating the measured charge to the continuous charge leads to the charge recovery according to:

$$\eta_{rec} = Q_m{}^{*}Q_{cont}^{-1} \quad (3)$$

When the charge recovery is larger than 1, it is more effective to operate the capacitive electrode in the charge–discharge mode, than the noncapacitive electrode in continuous mode. When it is equal to 1, than the charge–discharge operation of the capacitive electrode is just as effective as the continuous operation of the noncapacitive electrode. When the charge recovery is smaller than 1, it would have been more effective to operate a noncapacitive electrode in continuous mode.

Table 1
Charge and Discharge times [min] used during the experiments.

Ratio	Charging time [min] × total experiment time [min]$^{-1}$	
0.5	**0.6**	**Various**
10–10	5–10	5–20
15–15	10–20	60–90
20–20	30–60	90–120
30–30	60–120	90–150
60–60	n.d.	120–180

n.d.: Not determined.

3. Results and discussion

3.1. Electrochemical characterization of the bio-anode

The bio-anode was characterized by recording a polarization curve at day 32, 76 and 120 for each of the six cells. For each capacitive layer, the average current density of two cells during these three polarization curves can be found in Fig. 2. For each capacitive electrode, the current density increased throughout the whole range of measured anode potentials. The capacitive electrode with a thickness of 1.5 mm reached a maximum current density of 1.86 Am^{-2} at an anode potential of −0.250 V. The capacitive electrode with a thickness of 0.5 mm reached a maximum current density of 1.96 Am^{-2} and overall the highest current density was achieved by the capacitive electrode with a thickness of 0.2 mm and its maximum current density was 2.53 Am^{-2}. All capacitive bio-anodes showed very similar performance between the duplicates and also in the beginning, middle and end of operation, what means that they are really stable in their current density output.

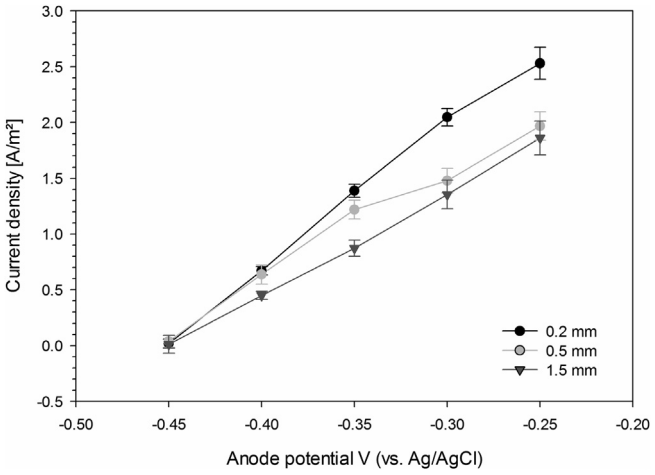

Fig. 2. Polarization curves obtained for the different capacitive electrodes for the anode potential range from −0.450 to −0.250 V. The thickness of the electrode has a clear influence on the performance of each capacitive electrode with 0.2 mm showing the best performance.

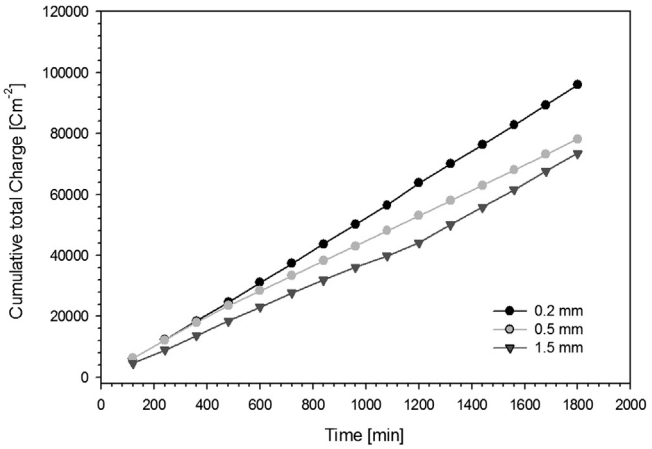

Fig. 3. Cumulative Total Charge of the capacitive electrodes during the charge–discharge experiment (60–60 min). This experiment shows the representative trend in behavior of the capacitive electrodes for all charge–discharge experiments.

3.2. Characterization of the capacitive layers

The capacitive electrodes were characterized for their surface properties using the BET-Analysis. Through the BET-Analysis the specific surface area of each electrode was determined. The results are in Table 2.

The BET-results show that with increasing thickness, the specific surface area of the capacitive electrode decreases. With the AFM the roughness of these capacitive electrodes was determined. The roughness is shown as the arithmetic average R_a in Table 2. The roughness of the capacitive layers also decreased with increasing thickness. The SEM-pictures, which were taken from these capacitive layers showed an even distribution of ACP and PVDF throughout the whole layer. No differences between the three different capacitive layers could be detected from the SEM-pictures.

3.3. Charge–discharge experiments

During the charge–discharge experiments, a period with open circuit (charging) was alternated with a period in which the anode potential was controlled at an anode potential of −0.300 V (discharging). The periods for charging and discharging were varied in different ratios between charging and discharging, according to the times given in Table 1. Representative graphs for the cumulative total charge (charging (60 min) and discharging (60 min)), calculated according to Equation (2) are shown in Fig. 3. Clearly, the capacitive electrodes performed very stable during the alternating conditions of the charge–discharge experiment: each charge/discharge step results in a similar increase in total charge, which is shown by a linear increase of the cumulative total charge in time. Furthermore, in accordance with the observations in the polarization curves, the capacitive electrode with a thickness of 0.2 mm performed best during this representative experiment. This capacitive electrode reached a cumulative total charge of 96013 cm^{-2}. The capacitive electrode with a thickness of 0.5 mm was the second best (78215 cm^{-2}) and the capacitive electrode with a thickness of 1.5 mm was the least performing electrode (73481 cm^{-2}).

Table 2
Specific surface area for each capacitive electrode.

	Norit DLC Super 30		
	0.2 mm	0.5 mm	1.5 mm
Specific surface area [m^2 g^{-1}]	942 ± 16.2	795 ± 20.4	742 ± 37.0
Surface roughness R_a [nm]	67.2	57	52.9

3.4. Relative charge recovery

The relative charge recovery was calculated for each charge–discharge experiment according to Equation (3). This relative charge recovery indicates the performance of the capacitive electrode during one charge–discharge cycle compared to the performance of a non-capacitive electrode during continuous operation in the same time. The relative charge recovery for the charge–discharge experiments with a ratio of 0.5 for the charging time vs. total cycle time is shown in Fig. 4. During the experiments with a shorter total cycle time, the capacitive electrode with a thickness of 1.5 mm had a higher relative charge recovery than the other capacitive electrodes. The relative charge recovery was close to 1, which means that it is as efficient to operate this capacitive electrode in the cycling mode with periods of an open electric circuit,

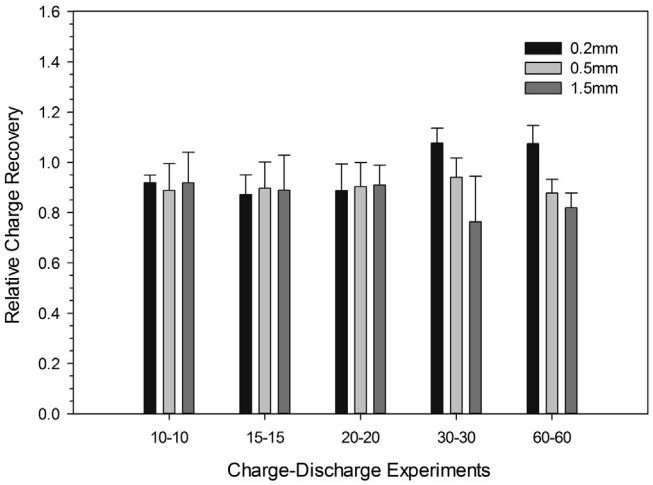

Fig. 4. The relative charge recoveries for each capacitive electrode during the charge–discharge experiments with the 0.5 ratio of charging time compared to the total cycle time.

than to operate a noncapacitive electrode continuously. Furthermore, the relative charge recovery of the capacitive electrode with a thickness of 1.5 mm decreased when the total cycle time increased. During the experiments with 20 min of charging and 20 min of discharging all the capacitive electrodes achieved the same relative charge recovery of 0.95. For the experiments with a longer total cycle time, the capacitive electrode with a thickness of 0.2 mm was outperforming the other capacitive electrodes (and the continuous operation of a noncapacitive electrode as well) as its relative charge recovery was as high as 1.15. For the 0.2 mm capacitive electrode, the relative charge recovery was increasing with increasing total experiment time. The relative charge recovery for the experiments with a ratio of charging time vs. total cycle time of 0.67 is in Fig. 5. The capacitive electrode with a thickness of 0.2 mm outperformed the other two electrodes throughout all these experiments, its relative charge recovery being larger than or equal to 1 throughout all these experiments. The highest relative charge recovery achieved by this electrode was 1.32. The relative charge recovery for the charge–discharge experiments with various ratios between charging and total cycle time is shown in Fig. 6. During all these experiments the capacitive electrode with a thickness of 0.2 mm again outperformed the other two electrodes, its relative charge recovery being larger than 1 during all these experiments. The maximum relative charge recovery was 1.35.

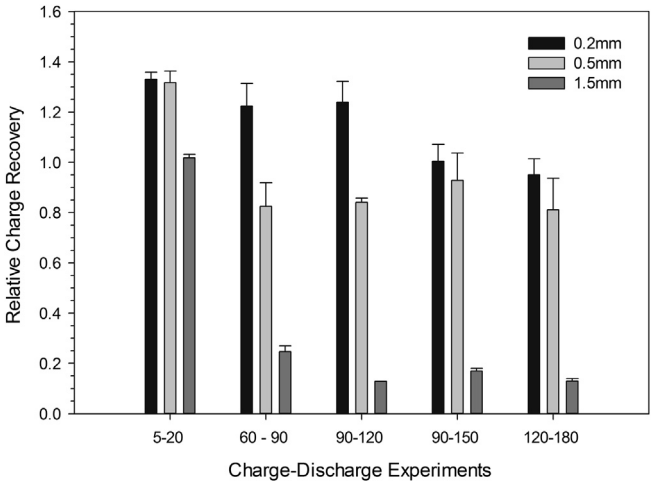

Fig. 6. The relative charge recovery of the capacitive electrodes during the charge–discharge experiments with various ratios of charging time compared to total cycle time.

3.5. Discussion

The effect of the thickness of the capacitive electrode on bioanode performance was determined during polarization curves and charge-discharge experiments. The capacitive electrodes had thicknesses of 0.2 mm, 0.5 mm and 1.5 mm. It was found that the electrode thickness clearly affected bioanode performance. During the polarization curves, the capacitive electrode with a thickness of 0.2 mm performed better than the other two thicker capacitive electrodes. Interestingly, performance decreased with increasing thickness of the capacitive layer, which is different from literature [13] where they found an increase in performance with increasing thickness of the electrode. The same relationship was found for the specific surface area of the capacitive electrodes in the BET-Analysis and for the average roughness of the capacitive layer surface in the AFM-pictures. The specific surface area decreased with increasing thickness of the capacitive electrode, giving the highest specific surface area of 942 m^2g^{-1} and the highest roughness of 67.2 nm for the capacitive electrode with a thickness of 0.2 mm. Therefore, it can be expected that the capacitive electrode with 0.2 mm thickness is the most efficient, since a higher specific surface area and a rougher surface structure offers more space for the growth of microorganisms. This is in accordance with the polarization curves (Fig. 2), where the capacitive electrode with a thickness of 0.2 mm achieved the highest current density.

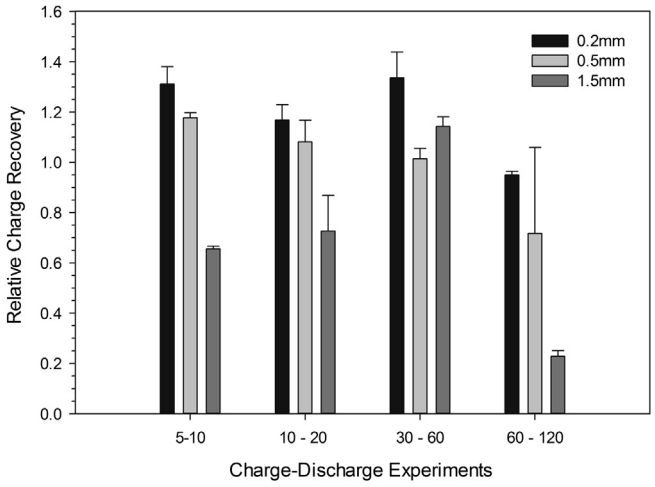

Fig. 5. The relative charge recovery of the capacitive electrodes during the charge–discharge Experiments with the ratio of 0.67 for charging time compared to the total cycle time.

During charge–discharge experiments and their related relative charge recoveries part of the difference can be related to the difference in specific surface area, although some small fluctuations can be seen in Figs. 4, 5 and 6. The part of the difference in performance, which cannot be related to the specific surface area, might be due to the difference in internal resistance in the capacitive electrodes. It is expected that with increasing thickness of the capacitive layer the transport resistance (resistance for transport of ions through the pores) is increasing [19]. Therefore the ions are transported much easier through the capacitive layer with a thickness of 0.2 mm compared to the capacitive layer with a thickness of 1.5 mm. This might be the reason why the capacitive electrode with a thickness of 1.5 mm is achieving lower current densities during the long charge–discharge cycles compared to the continuous operation in the polarization curves. The capacitive electrode with a thickness of 1.5 mm experienced some instability in the performance during the long charge–discharge cycles. With increasing charge–discharge cycle times this effect got stronger which is also reflected in the relative charge recovery of this electrode which was lower (see Figs. 5 and 6) than during shorter experiment cycle times.

The capacitive electrode with a thickness of 0.5 mm performed stable throughout both the polarization curves and the charge–discharge experiments. It was the most stable operating electrode. The capacitive electrode with a thickness of 0.2 mm performed best throughout most of the experiments, but its performance was fluctuating (see Fig. 6). Overall, during most of the charge–discharge experiments, the capacitive electrode with a thickness of 0.2 mm achieved the best relative charge recovery. The achieved relative charge recoveries were close to or larger than 1, which means that, depending on the charge–discharge cycling time, the 0.2 mm capacitive electrode produced more charge than the noncapacitive electrode at continuous operation.

The highest achieved relative charge recovery was 1.4, meaning a 40% better performance compared to the noncapacitive electrode. In the previous study [12] the charge recovery was 52% higher than the noncapacitive electrode. But in that study the measured charge (Q_m) was only related to the charge expected from the noncapacitive electrode during the discharging period t_d and not from the total experimental time t_o (see Equation (3)). Recalculating the earlier found charge recovery increase of 52% to the relative charge recovery, would lead to an increase of only 4%. Therefore the performance of the capacitive electrode has been increased by 36%, by decreasing its thickness from 0.5 mm to 0.2 mm.

4. Conclusion

The influence of the thickness of the capacitive layer on the performance of these capacitive bioanodes was investigated in an MFC. Polarization curves, charge–discharge experiments and the relative charge recovery showed that the total current density and the amount of stored charge and therefore the performance increased in the order: capacitive layer 1.5 mm < capacitive layer 0.5 mm < capacitive layer 0.2 mm. This increase in performance is similar to the increase in specific surface area, but this is not the only factor affecting the performance. It is assumed that the transport resistance is increasing with increasing thickness of the capacitive layer and therefore limiting the current output of the thicker electrodes. Further studies might deliver more insights on the factors which are affecting the power output of the capacitive bioanodes. Also variations in the properties of the capacitive layer, like the type of activated carbon powder and the type of binder, might lead to further increase in bio-anode performance.

Acknowledgments

This work was performed in the TTIW-cooperation framework of Wetsus, Centre of Excellence for Sustainable Water Technology (www.wetsus.nl). Wetsus is funded by the Dutch Ministry of Economic Affairs, the European Union European Regional Development Fund, the Province of Fryslân, the city of Leeuwarden and by the EZ-KOMPAS Program of the "Samenwerkingsverband Noord-Nederland". The authors like to thank the participants of the research theme "Resource Recovery" for the fruitful discussions and their financial support.

References

[1] W. Moomaw, in: IPCC Scoping Meeting on Renewable Energy Sources – Proceed (2008), pp. 3–32.
[2] G. Berndes, M. Hoogwijk, R. van den Broek, Biomass Bioenergy 25 (1) (2003) 1–28.
[3] P. Aelterman, et al., Water Sci. Technol. 54 (8) (2006) 9–15.
[4] R.A. Rozendal, et al., Trends Biotechnol. 26 (8) (2008) 450–459.
[5] B.E. Logan, et al., Environ. Sci. Technol. 40 (17) (2006) 5181–5192.
[6] W.F. Pickard, A.Q. Shen, N.J. Hansing, Renewable Sustainable Energy Rev. 13 (8) (2009) 1934–1945.
[7] A. Dewan, H. Beyenal, Z. Lewandowski, Environ. Sci. Technol. 43 (12) (2009) 4600–4605.
[8] Y. Kim, et al., Energy Environ. Sci. 4 (11) (2011) 4662–4667.
[9] F. Grondin, M. Perrier, B. Tartakovsky, J. Power Sources 208 (0) (2012) 18–23.
[10] P. Liang, et al., Environ. Sci. Technol. 45 (15) (2011) 6647–6653.
[11] M.C. Hatzell, Y. Kim, B.E. Logan, J. Power Sources 229 (0) (2013) 198–202.
[12] A. Deeke, et al., Environ. Sci. Technol. 46 (6) (2012) 3554–3560.
[13] C. Emmenegger, et al., J. Power Sources 124 (1) (2003) 321–329.
[14] K.-C. Tsay, L. Zhang, J. Zhang, Electrochim. Acta 60 (0) (2012) 428–436.
[15] P.W. Atkins, Physical Chemistry, vol. 1, VCH Wiley Interscience, Weinheim, 1990.
[16] G. Haugstad, Atomic Force Microscopy, vol. 1, VCH Wiley, Weinheim, 2012.
[17] A. ter Heijne, H.V.M. Hamelers, C.J.N. Buisman, Environ. Sci. Technol. 41 (11) (2007) 4130–4134.
[18] B.E. Logan, J.M. Regan, Environ. Sci. Technol. 40 (17) (2006) 5172–5180.
[19] T.H.J.A. Sleutels, et al., Int. J. Hydrogen Energy 34 (24) (2009) 9655–9661.